Appendix: Aspects of data treatment for transverse μSR

B D Rainford

University of Southampton, England

1 Introduction

My main message is that in μSR experiments we are always fighting with poor counting statistics , so we must do nothing to our data which makes matters worse, and we should do whatever we can to extract the most from what we have. The approach is geared to the typical set-up encountered at the pulsed muon beams at ISIS, but is readily generalised to other situations.

A typical ISIS μSR data set.

A data set collected on the MuSR or EMU spectrometers at ISIS consists typically of 32 histograms containing between 1000 to 2000 time channels; the channel widths are 8 or 16ns. These widths are chosen to match the width of the muon pulse, which is of order 70ns (FWHM). As an example let us consider a data set of 1500 channels, with channel width 16ns. The total time window for data collection is then 0 to 24μs. As the muon lifetime τ_μ is 2.2μs, the end of the time window corresponds to $10.9\tau_\mu$, by which time the initial decay count rate will have dropped by a factor $\exp(-10.9) = 2 \times 10^{-5}$! Fortunately the background at ISIS is very low, so it is still possible to collect data out to these times, though the statistics will inevitably be poor.

To develop a feeling for counting statistics, let us consider a standard silver run, measured for one hour (this is a typical duration for a measurement), corresponding to $2{\times}10^7$ events (20"Mev"), summed over all 32 histograms. The counts in channel n of detector j are given by:

$$C_j(t_n) = N_j^0 \Delta t \exp(-t_n/\tau_\mu)[1 + A_j \cos(\omega_L t_n - \phi_j)] \quad (1)$$

where A_j is the asymmetry parameter (typically $A_j = 0.23$ at ISIS), ϕ_j is the phase, Δt is the channel width, N_j^0 is the initial count rate, $\omega_L = \gamma B$ is the muon Larmor precession

frequency for an applied field B and the gyromagnetic ratio $\gamma/2\pi = 135.54$MHz/tesla. Ignoring the oscillatory term in (1) for the moment, we can sum over all time channels, to estimate the total number of events per histogram:

$$\sum_n C_j(t_n) \approx \int_0^\infty N_j^0 \exp(-t/\tau_\mu)dt = C_j(0)\tau_\mu/\Delta t$$

Taking the total counts to be $2\times10^7/32$, then we find that $C_j(0)$, the counts at the start of each histogram, to be about 4500. The statistical error in this count is $\sqrt{C_j(0)} = 67$. Of all the events, we are only interested in that portion associated with the asymmetry, $A_jC_j(0) = 0.2\times4500 = 900$ counts. It follows that the statistical error in the asymmetry, at the beginning of the histogram, where we have the highest count-rate, is only $67/900 \equiv 7.4\%$. This is not very impressive! And at longer times it will be worse. If we wanted, say, 1% statistics on the initial asymmetry we would need $\sqrt{C}/(0.2\text{C}) = 0.01$, corresponding to $C_j(0) = 2.5\times10^5$ counts, or a total of 10^9 events in all 32 histograms! This would mean running for 55 hours on ISIS!

The moral is that in the average μSR experiment we are dealing with quite poor counting statistics. This is largely a consequence of (i) the signal being associated with only 20% of the total counts, and (ii) the short lifetime of the muon. Clearly it is essential, when analysing μSR data, to make every event count and to avoid any process which throws away information, e.g. grouping detectors with different phases together; this might be useful for summary purposes, or plotting data during an experiment, but it will reduce the effective asymmetry, and is therefore a bad thing for the ultimate analysis of μSR data.

2 Determination of instrumental parameters

2.1 Phases and start time

The time t_n in (1) is measured with respect to the start time t_0, when the muons arrive in the sample: $t_n = n\Delta t + t_0$. The effective phase of the oscillatory term is therefore $\psi_j = \phi_j - \omega_L t_0 = \phi_j - \gamma B t_0$. All detectors should have a common value of t_0. This can be determined by measuring silver spectra for several different transverse fields B, fitting the count-rate to (1) to determine the effective phases ψ_j, then plotting these as a function of B. The plots give straight lines which, when extrapolated to zero field, give the true phases ϕ_j. The start time t_0 can be extracted from the gradients. Alternatively the phases ψ_j can be determined for different assumed values of t_0, then plots of $\psi_j(t_0)$ for different fields should intersect at the true value of t_0.

Fitting of (1) to a silver spectrum in order to determine the phases is straightforward: it can be implemented by a linear least squares method, since (1) can be written as: $C_j^t = \alpha_j F_t + \beta_j G_t$, with $\alpha_j = \sin\phi_j$ and $\beta_j = \cos\phi_j$. Then following the usual approach

$$\chi^2 = \sum_t \left[C_j^t - \alpha_j F_t - \beta_j G_t\right]^2 / \sigma_{jt}^2$$

and the values of α_j and β_j can be found by minimising χ^2 in the normal way.

2.2 Dead time corrections

The count-rate equation (1) assumes a linear detector response, *i.e.* that the number of detected events in a given time channel is simply proportional to the number of decay positrons at that time. In general this is a reasonable assumption for low count rates, but at high count-rates we have to correct for the "dead time" of the detector. This arises because the counting chain cannot respond to two events that come very close together: the counter is "dead" for a time τ_d after the first positron is detected. Since for μSR data the count rate is initially high and then falls with time, the effect of the dead time will be biggest at early times, and will become negligible at later times. The corrections for dead time can be derived from a standard zero field silver run, preferably one with good statistics.

To see the effect of dead time, let us consider a simple case, where $N(t)$ represents the ideal counting rate and $M(t)$ is the recorded counting rate. In a single time channel of width Δt the detector will be dead for a time $M(t)\Delta t\,\tau_d$, so the measured count in this time channel will be $M(t)\Delta t = N(t)\Delta t[1 - M(t)\tau_d]$. It follows that the recorded count rate is

$$M(t) = \frac{N(t)}{1 + N(t)\tau_d}. \tag{2}$$

Clearly for $N(t)$ small and $N(t)\tau_d \ll 1$, then $M(t) \approx N(t)$. However when the count-rate is very high, the measured counts tend to the limiting value $M(t) = 1/\tau_d$. To determine the dead times for each detector, the reciprocal of the measured counts in a zero field silver run can be plotted against the reciprocal of $N(t)$ with $N(t) = N_0 \exp(-t/\tau_\mu)$. From (2) it can be seen that a straight line should result with intercept τ_d:

$$\frac{1}{M(t)} = \frac{1}{N(t)} + \tau_d.$$

The value of the dead time can then be extracted from a least squares fit to the straight line. If only a transverse field silver run is available, the same procedure can be used, but in this case the ideal counts are as given in Equation (1). In practice for a typical ISIS count rate the dead time corrections at short times are about 5% or less.

3 Analysis of μSR spectra

There are two perspectives for the interpretation of transverse field μSR spectra:

- **Case (a)**: The muon spins precess at a unique frequency ω_L, but their polarisation decays with time due to the muons' interaction with static or dynamic fluctuations in its environment. In metals the precession frequency ω_L might be shifted slightly from the value γB_{ext} (Knight shift), reflecting an enhanced susceptibility at the muon site in the sample.

- **Case (b)**: The muons at different sites see a distribution of internal fields, and therefore precess at different rates. This is the case, for example, in the mixed state of superconductors.

We will consider these situations in turn in Sections 3.1 and 3.3, following. In both cases there are special techniques available which are useful for tackling data comprising multiple histograms.

3.1 Modelling the depolarisation in the time domain: case (a)

If the muons precess at a common frequency ω_L, but their polarisation decays with time, the counts in the n-th time channel of the j-th detector can be written:

$$C_j(t_n) = N_j^0 \Delta t \exp(-t_n/\tau_\mu)[1 + A_j P_x(t_n) \cos(\omega_L t_n - \phi_j)]. \quad (3)$$

$P_x(t)$ describes the decay of the muon polarisation. The form of this decay depends on the physics of the muon's interaction with its environment. In the limit of fast temporal fluctuations of the local field or of rapid hopping of the muon from site to site it can be shown that $P_x(t) = \exp(-\lambda t)$: this is traditionally (and confusingly) called "Lorentzian damping" because this limit is identical to the limit of strong motional narrowing in NMR, where the line-shape (equivalent to the Fourier transform of $P_x(t)$), is indeed a Lorentzian function. In the limit of slow temporal fluctuations, but where there is a Gaussian distribution local fields (inhomogeneous broadening) it is readily shown that $P_x(t) = \exp(-\sigma^2 t^2)$. Other functions in the literature, e.g. the Abragam function, are designed to describe circumstances between these two limiting cases. The point is that the shape of the envelope of the decaying polarisation gives information about the physics of the interaction at the muon site, which can be described by an analytical function with a few parameters (*e.g.* λ or σ in the above expressions). Analysis of the data is then a simple matter of least squares fitting the expression (3) to the data, with the appropriate form of $P_x(t)$. Following our dictum in Section 1, we should, if possible, fit all the histograms ($j = 1, \ldots 32$) at the same time, without grouping them together, after making necessary corrections for dead times. In this case there will be three instrumental parameters for each histogram, namely N_j^0, A_j and ϕ_j as well as the parameters describing the polarisation $P_x(t)$. In practice it is best to predetermine the phases as described in Section 2.1, using a standard silver run, since the phases might not be well determined in a fit to the data, especially when the polarisation is rapidly damped. Fitting 32×1500 time channels with 65 parameters might seem like a tall order, but computing power is cheap compared to the cost of doing μSR experiments. In the next section we show a way of combining multiple histograms without losing information, which reduces considerably the effort of fitting models to the data.

3.2 Combining multiple histograms

We need a technique that allows us to condense a data set comprising multiple (*e.g.* 32) histograms without losing information. The following method is based on unpublished work by G J Daniell and has been implemented in a practical program for ISIS data by W R Dickson. Starting from the raw data, as described by (3) above, it is straightforward to extract the exponential decay term due to the muon lifetime and the uniform contribution. This yields the component of the signal that oscillates about zero:

$$d_j(t_n) = N_j^0 \Delta t A_j P_x(t_n) \cos(\omega_L t_n - \phi_j) = D_j(t) \cos(\omega_L t_n - \phi_j) \quad (4)$$

for each histogram, $j = 1, \ldots J$ and time channel, $n = 1, \ldots N$. We also have the corresponding variances $\sigma_j(t_n)$ in the $d_j(t_n)$. Now we can project all the data onto a given phase by taking a linear combination of all the histograms. Suppose we choose a value of zero for the phase: we can define a function $X(t)$ such that

$$\begin{aligned} X(t_n) = D_j(t_n)\cos(\omega_L t_n) &= \sum_j x_j d_j(t_n) \\ &= \sum_j x_j D_j(t_n)\left\{\cos(\omega_L t_n)\cos(\phi_j) - \sin(\omega_L t_n)\sin(\phi_j)\right\}. \end{aligned} \quad (5)$$

Obviously this identity is true if the weights x_j are chosen so that $\sum_j x_j \cos\phi_j = 1$ and $\sum_j x_j \sin\phi_j = 0$. We can use these two conditions as constraints in a least-squares minimisation of the square of the variance of our new histogram $X(t_n)$ by using Lagrange multipliers. We then have to minimise

$$\sum_j \sum_n x_j^2 \sigma_j^2(t_n) - \lambda\left[\sum_j x_j \cos\phi_j - 1\right] - \mu \sum_j x_j \sin\phi_j$$

with respect to the weights x_j , where λ and μ are the Lagrange multipliers. This leads to the result:

$$x_j = \frac{\lambda\cos\phi_j + \mu\sin\phi_j}{2\sum_n \sigma_j^2(t_n)} \quad (6)$$

We can now use the two constraints equations to determine λ and μ. In order to simplify the resulting expression let us introduce the following notation for the sums involved:

$$\overset{ss}{\sum} = \sum_j \sin^2(\phi_j)/\Delta_j; \qquad \overset{sc}{\sum} = \sum_j \sin(\phi_j)\cos(\phi_j)/\Delta_j; \qquad \overset{cc}{\sum} = \sum_j \cos^2(\phi_j)/\Delta_j;$$

where

$$\Delta_j = 2\sum_n \sigma_j^2(t_n).$$

The final result for the weights x_j is then:

$$x_j = \Delta_j^{-1}\left\{\cos\phi_j - \sin\phi_j \overset{sc}{\sum}/\overset{ss}{\sum}\right\} \Big/ \left\{\overset{cc}{\sum} - \left(\overset{sc}{\sum}\right)^2/\overset{ss}{\sum}\right\} \quad (7)$$

We can now choose a second orthogonal value for the phase and define another function $Y(t)$ such that:

$$Y(t_n) = D_j(t_n)\sin(\omega_L t_n) = \sum_j y_j d_j(t_n) \quad (8)$$

The weights y_j are now chosen so that $\sum_j y_j \cos\phi_j = 0$ and $\sum_j y_j \sin\phi_j = -1$. Following the same method we find that the weights are given by:

$$y_j = \Delta_j^{-1}\left\{-\sin\phi_j + \cos\phi_j \overset{sc}{\sum}/\overset{cc}{\sum}\right\} \Big/ \left\{\overset{ss}{\sum} - \left(\overset{sc}{\sum}\right)^2/\overset{cc}{\sum}\right\} \quad (9)$$

By combining all J histograms with the appropriate weights x_j and y_j we can project out two histograms with orthogonal phases. These contain all the original information

and the variance of each is of order $1/J$ times that of a single histogram. These projections of the data are very convenient for displaying the "real" information content in the data and for modelling the form of the depolarisation, as discussed in section 3.1 above, since now there are only two amplitudes to be determined, besides the parameters describing the model for $P_x(t)$. It is also possible to combine the two histograms with orthogonal phases to give a signal proportional to $P_x(t)$ directly, without any oscillating component.

3.3 Transforming data into the frequency domain: case (b)

If the muon sees a distribution of internal fields the counts in each detector will be:

$$C_j(t_n) = N_j^0 \Delta t \exp(-t_n/\tau_\mu)[1 + A_j F_j(t_n)] \tag{10}$$

where

$$F_j(t_n) = \int_0^\infty F(\omega) \cos(\omega t_n - \phi_j)\, d\omega.$$

The function $F(\omega)$ gives the distribution of precession frequencies, which maps directly onto the distribution of internal fields through the gyromagnetic ratio: $\omega = \gamma B$. The problem is how to extract $F(\omega)$ from the data. This is clearly a Fourier transform problem, but standard Fourier methods have some drawbacks, in particular:

1. The poor statistical accuracy of the μSR data at long times leads to very noisy transforms. Of course there are standard techniques for coping with this, for example use of window functions ("apodisation"). There is a large literature on how to choose the optimum window function, however whichever one is chosen, they all involve throwing away data, and some deterioration of the frequency resolution.

2. We have a problem of how to derive a unique frequency spectrum $F(\omega)$ from 32 separate histograms, with different phases ϕ.

Recently this problem has been tackled by Rainford and Daniell (1994) using the Maximum Entropy method. This technique has been widely used to deal with a range of inverse problems in fields such as radio astronomy, geophysics and image reconstruction (including processing images from the Hubble telescope to correct for the aberrations in the mirror) etc. Applied to the present problem it has many advantages:

- It uses all the data available, but allows a unique frequency spectrum to be determined from multiple histograms.
- The frequency spectrum derived is necessarily positive.
- There are no prior assumptions about the form of $F(\omega)$.
- It gives the most uniform (N.B. not smoothest) distribution consistent with the data.
- It is possible to include convolution with the muon pulse shape.
- The ultimate frequency resolution can be achieved.

Details of the method will not be given here, since they are discussed in Lee (1993). Briefly the entropy S is defined in the information theoretic sense as

$$S = \sum_k (p_k/b_k) \log(p_k/b_k)$$

where the $\{p_k\}$ represent the heights of the bins in the histogram representing the frequency spectrum. The b_k represent the default values which give a scale to the magnitudes of the p_k. In practice the default is taken to be a flat level, independent of k. Starting from this featureless default level, the ME algorithm searches for a solution which maximises $S - \lambda\chi^2$ where λ is a Lagrange multiplier. Initially λ is chosen so that the algorithm puts most effort into minimising χ^2. with the aim of reducing its value to be equal to the number of data points. In the later stages the value of λ is altered to concentrate on maximising the entropy. The advantage of the technique is that it tackles the forward problem, *i.e.* generates a frequency spectrum which is then transformed, as in (10), to give the measured counts in each histogram, which are then compared to the measured values. This facilitates the incorporation of any transformation between the frequency domain and the time domain, e.g. convolution with the pulse shape of the muon bursts. The resulting frequency spectra produced by the method are impressive. For example Figure 1 shows the frequency spectrum for silver, which is very close to a delta function, as we might expect. This technique has been widely used by a number of groups (Lee et al 1993) to study the mixed state of super- conductors. The distribution of internal fields in this case is highly asymmetric, with a high field tail extending up to B_{c2}, resulting from the flux lattice structure. The asymmetry of the μSR frequency distribution can therefore be used as an indicator of a well ordered flux lattice.

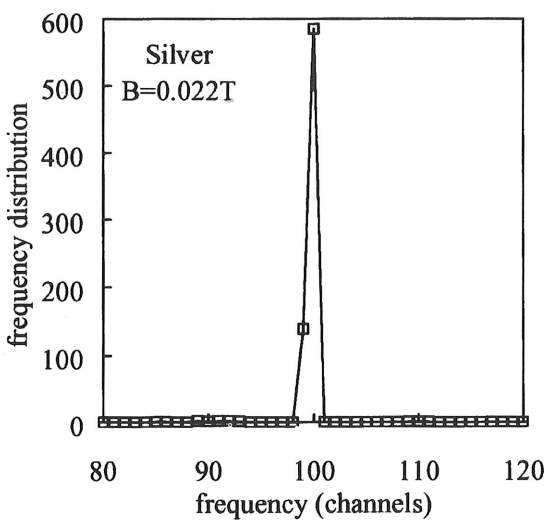

Figure 1. *Frequency spectrum from a Maxent analysis of a silver data set with B_{ext}= 220 gauss. The width of one frequency channel corresponds to 30.5kHz or 2.25 gauss. The small feature to the left of the main peak near channel 92 is due to muons stopping in the end of a collimator.*

4 Limitations to the transverse μSR method

4.1 Effect of finite muon lifetime

Clearly μSR would not work if the muon did not decay! However the finite lifetime of the muon means that we can only collect useful data for, perhaps, five muon lifetimes (data at longer times are useful if we are prepared to count for a long time to improve the statistics). This immediately implies a limit to the frequency resolution of the transverse μSR technique. To see this consider the standard approach from the theory of discrete Fourier transforms (DFT): in a DFT of data comprising n channels with channel width Δt the frequency resolution Δf is simply $1/n\Delta t = 1/T$, *i.e.* the reciprocal of the total time for which data has been collected. If we take $T = 5\tau_\mu = 11\mu$sec, then $\Delta f \approx 90$kHz. Transforming this from frequency to magnetic field, using the gyromagnetic ratio of the muon, the resolution in magnetic field is about 0.7mT or 7 gauss. Note that this is a fundamental restriction, no matter how good our instrumentation or data analysis.

4.2 Effect of finite pulse width

The time structure of the muon beam at ISIS reflects that of the proton pulses at the production target, i.e. two pulses of width 70ns (FWHM) with a separation of 340ns. The repetition rate is 50Hz. The pulses are further smeared by the 26ns lifetime of the parent pions. The first of the double pulses is split between the two μSR instruments EMU and DEVA, while the second pulse passes on to the MuSR instrument. It follows that the time dependent count-rate (3) or (10) should be convoluted with the pulse shape of the incident muon beam. This will have a significant effect only when there are variations in the count-rate on a time scale comparable to the pulse width. There are two particular cases where this might be important: (i) when the Larmor precession frequency is high, and (ii) where there is rapid decay of the muon polarisation. Let us consider these in turn.

Upper limit to the external field

Suppose that we take the muon pulse shape to be a gaussian: $W(t) = \exp(-t^2/\tau_w^2)$. This is not strictly correct: a better approximation at ISIS is an inverted parabola, describing the proton pulse, convoluted with a decaying exponential, in order to account for the pion lifetime component. However a simple gaussian simplifies the result greatly. If we are studying a material like silver which is weakly damped, the resulting signal would be the convolution of the "ideal" signal $[1+A\cos(\omega_L t)]$ with $W(t)$. Here A is the ideal asymmetry and ω_L is the Larmor precession frequency, as usual. It is straightforward to show that the effect of the convolution is to reduce the asymmetry to a value $A\exp[-(\omega_L\tau)^2/4]$. The reduction in the asymmetry with applied field is shown in Figure 2 for different values of the pulse width τ_w. It follows that the asymmetry falls to $1/e$ of its ideal value at an applied field B given by $(\omega_L/2) = (\gamma/2)B_{1/e} = 1/\tau_w$. For a pulse width of 70ns (FWHM) the value of $\tau_w \approx 42$ns, and the corresponding field $B_{1/e}$ is 560 gauss. The reduced asymmetry resulting from high Larmor precession rates degrades the signal to noise, as is clear from the discussion in Section 1 above.

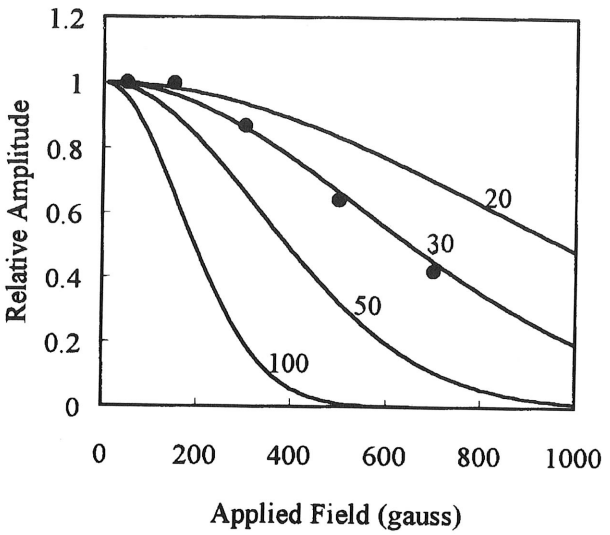

Figure 2. *Variation of the asymmetry with external field due to the finite width of the muon pulses, after Nagamine and Yamakazi. The numbers on the curves give the value of τ_w in nanoseconds.*

Upper limit to damping rate

If the damping rate were very high then the muon polarisation $P_x(t)$ would fall to a small value within one Larmor precession period, or in the extreme case, within the muon pulse width. In the latter case, Lorentzian damping would only be visible for values of the damping rate smaller than $\lambda_{\max}$ given by, say, $\exp(-\lambda_{\max}\tau_w) \approx e^{-1}$, that is we suppose that the muon polarisation decays by $1/e$ over the duration of the muon pulse. Using the above value $\tau_w = 42$ns gives a value for $\lambda_{\max} \approx 24\mu s^{-1}$. However to extract such a value from real data would require a very accurate knowledge of the pulse shape and the start times for each histogram, and a careful deconvolution procedure. Notice that the situation at ISIS for measuring heavily damped signals is very much improved now that single pulses are used: with the same criterion as above for a double pulse of muons separated by 320ns we find a value of $\lambda_{\max}$ of only $2.9\mu s^{-1}$. In practice deconvolution of the pulse shape is necessary to extract reliable values of λ for damping rates greater than 3–$5\mu s^{-1}$, but the extra data analysis effort required is well justified.

References

Lee S L *et al.* , 1993, *Phys Rev Lett* **71** 3862
Rainford B D and Daniell G J, 1994, *Hyperfine Interactions* **87** 1129

Participants

Addresses corrected at end April 1999

- Dr Christof Aegerter
  Dept of Physics 0319
  Univ of California San Diego;
  9500 Gilman Drive;
  La Jolla,
  Ca 92093; USA
  e-mail: aegerter@physics.ucsd.edu

- Dr Daniel-Aurelian Andreica
  Institute of Particle Physics
  ETHZ, IPP/ETHZ, WLGA/C21
  5232 Villigen-PSI, SWITZERLAND
  e-mail: daniel.andreica@psi.ch

- Mr Cameron Ager
  School of Physics and Astronomy
  University of St Andrews
  St Andrews KY16 9SS UK
  e-mail: ca8@st-andrews.ac.uk

- Dr Michel Ain
  Lab Leon-Brillouin
  CEA-Saclay
  91191 Gif/Yvette Cedex, FRANCE
  e-mail: ain@cea.fr

- Dr Helena Alberto
  Physics Department
  University of Coimbra
  P-3000 Coimbra, PORTUGAL
  e-mail: lena@gemini.ci.uc.pt

- Dr Dimitrios Anagnostopoulos
  Dept of Computer Science
  University of Ioannina, GREECE
  e-mail: danagno@mail.cern.ch

- Mr Jonathon Armitage
  School of Physics and Astronomy
  University of St Andrews
  St Andrews, KY16 9SS UK
  e-mail: jgma@st-andrews.ac.uk

- Mr Tomasz Blach
  Griffith University
  School of Science
  Kessels Road, Nathan Q4111
  AUSTRALIA
  e-mail: T.Blach@sct.gu.edu.au

- Dr Joacim Bogner
  Institut fur Angewandte und Technische Physik
  Technische Univ Wien
  Wiedner Haupstr. 8-10, A-1040,
  Wien AUSTRIA
  e-mail: bogner@atp3100.tuwien.ac.uk

- Professor Jess Brewer
  Department of Physics
  University of British Columbia
  Vancouver, BC, V6T 2A6, CANADA
  e-mail: brewer@physics.ubc.ca

- Mr Craig Brown
  National Institute of Standards and Technology
  Githersburg
  MD 20899, USA
  e-mail: craig@rrdjazz.nist.gov

- Mr Shannon Brown
  School of Physics and Astronomy
  University of St Andrews
  St Andrews, KY16 9SS
  e-mail: sb10@st-and.ac.uk

- Dr Ian Campbell
  Physiques des Solides
  Université Paris Sud
  91405 Orsay, FRANCE
  e-mail: campbell@lps.u-psud.fr

- Professor Steve Cox
  ISIS Facility
  Rutherford Appleton Laboratory
  Chilton, Didcot, OX11 0QX, UK
  e-mail: sfjc@isise.rl.ac.uk

- Dr Gabriel Cuello
  Inst de Estructa de la Materia-CSIC,
  Serrano 123, E-28006
  Madrid, SPAIN
  e-mail: emcuello@iem.csic.es

- Professor Robert Cywinski
School of Physics and Astronomy
University of St Andrews
St Andrews, KY16 9SS, UK
e-mail: rc7@st-and.ac.uk

- Miss Judith Dann
School of Physics and Astronomy
University of St Andrews
St Andrews, KY16 9SS, UK
e-mail: jad4@st-and.ac.uk

- Mr Morgan Dawdy
2339 Spyglass Summit
High Ridge, MO 63049
USA
e-mail: morgan.dawdy@amd.com

- Dr Cesar De La Fuente
Dpto de Fisica de la
Materia Condensada,
Universidad de Zaragoza
Pedro Cerbuna 12, 50009 Zaragoza
SPAIN
e-mail: cesar@posta.unizar.es

- Dr Roberto De Renzi
Dipartimento di Fisica
Universita di Parma
1-43100, Parma, ITALY
e-mail: roberto.derenzi@pr.infn.it

- Dr Philip A Donnelly
Department of Physics and Astronomy
University College London
Gower Street, London WC1E 6BT, UK
e-mail: p.donnelly@ucl.ac.uk

- Dr Gordon Eaton
ISIS Facility
Rutherford Appleton Laboratory
Chilton, Didcot, OX11 0QX, UK
e-mail: ghe@isise.rl.ac.uk

- Mr Pedro Estrela
Van der Waals-Zeeman Institute
Univ of Amsterdam
Valckenierstraat 65, 1018 XE
Amsterdam, THE NETHERLANDS
e-mail: estrela@phys.uva.nl

- Mr Sandro Fanesi
Dipartimento Di Fisica
University of Parma
Viace Delle Scienze
C-43100 Parma, ITALY
estrela@wins.uva.nl

- Mr Julio Juan Fernandez-Sanchez
C/o Dr S Lee,
School of Physics and Astronomy
University of St Andrews
St Andrews, KY16 9SS, UK
e-mail:julioj@icmm.csic.es

- Dr Henryk Figiel
Department of Solid State Physics
University of Mining and Metallurgy
Av. Mickiewicza 30,
30-059 Cracow POLAND
e-mail: figiel@uci.qgh.edu.pl

- M Victorino Franco
Dpto. Fisica de la Materia Condensada
Sevilla University, PO Box 1065
41080 Sevilla, SPAIN
e-mail: vfranco@cica.es

- Dr Frederica Galli
Dipartimento Di Fisica
University of Parma
Viace Delle Scienze
43100 Parma, ITALY
e-mail: fgalli@prix7.pr.infn.it

- Dr Jose-Luis Garcia-Munoz
Inst de Materiales de Barcelona-CSIC
Campus Univ.Autonoma de Barcelona
E-08193, Bellaterra, SPAIN
e-mail: garcia.munoz@icmab.es

- M Fatih Gulener
Universite Paris-Sud
Batiment 510
Centre Universitaire
91405 Orsay CEDEX, FRANCE
e-mail:gulener@lps.u-psud.fr

- Dr Adrian Hillier
School of Physics and Astronomy
University of St Andrews
St Andrews, KY16 9SS, UK
e-mail: adh@st-and.ac.uk

- Mr Gareth Hopkins
School of Chemical Sciences
University of East Anglia
Norwich NR4 7TJ, UK
e-mail: g.hopkins@uea.ac.uk

- Dr Upali Jayasooriya
School of Chemical Sciences
University of East Anglia
Norwich NR4 7TJ, UK
e-mail: u.jayasooriya@uea.ac.uk

- Professor Klaus Jungmann
Physikalisches Institut der Universitaet Heidelberg
Philosophenweg 12
69120 Heidelberg, GERMANY
email: jungmann@physi.uni-heidelberg.de

- M Carlo Kaiser
IRI Delft University of Technology
Mekelweg 15, NL 2629 JB Delft
THE NETHERLANDS
e-mail: kaiser@iri.tudelft.nl

- Dr Czeslaw Kapusta
University of Mining and Metallurgy
Department of Solid State Physics
30-059 Cracow, POLAND
e-mail: kapusta@uci.agh.edu.pl

- Mr Paul Kealey
School of Physics and Astronomy
University of Birmingham
Edgbaston, Birmingham, B12 5TT, UK
e-mail: P.G.Kealey@bham.ac.uk

- Mr Ronald J Keizer
Van der Waals-Zeeman Institute
Univ of Amsterdam, Valckenierstraat 65
1018 XE Amsterdam,
THE NETHERLANDS
e-mail: rjkeizer@phys.uva.nl

- Dr Susan Kilcoyne
School of Physics and Astronomy
University of St Andrews
St Andrews, KY16 9SS, UK
e-mail: shk@st-and.ac.uk

- Dr Philip King
ISIS Facility
Rutherford Appleton Laboratory
Chilton, Didcot, OX11 0QX, UK
e-mail: p.j.c.king@rl.ac.uk

- Mr Waclaw Kocemba
University of Mining and Metallurgy
Department of Solid State Physics
30-059 Cracow, POLAND
e-mail: kocemba@uci.agh.edu.pl

- Dr Alexander Kolesnikov
Department of Physics
UMIST, PO Box 88
Manchester, M60 1QD, UK
e-mail: A.Kolesnikov@umist.ac.uk

- Dr. Alexandros Lappas
Institute of Electronic Structure and Laser (IESL)
Foundation for Research and Technology - Hellas (FORTH)
P.O. Box 1527
Heraklion 71110
Crete, GREECE
e-mail: lappas@iesl.forth.gr

- Dr Steve Lee
School of Physics and Astronomy
University of St Andrews
St Andrews, KY16 9SS, UK
e-mail: sl10@st-and.ac.uk

- Dr Jichen Li
Department of Physics
UMIST, PO Box 88
MANCHESTER, M60 1QD, UK
e-mail: j.c.li@umist.ac.uk

- Ms Anna Llobet
Lab. Louis Neel (CNRS)
25 Avenue des Martyrs
38042 BP 166 Grenoble
Cedex 9, FRANCE
e-mail: llobet@labs.polycnrs-gre.fr

- Dr James Lord
ISIS Facility
Rutherford Appleton Laboratory
Chilton, Didcot, OX11 0QX, UK
e-mail: j.s.lord@rl.ac.uk

- Mr Brendon Lovett
Kamerlingh-Onnes Laboratorium
PO 5404
2300 RA
Leiden
The Netherlands
Email: b.lovett1@physics.ox.ac.uk

- Ms Marcy Anne Lumsden
  Dept of Physics and Astronomy
  McMaster University
  1280 Main St. W.
  Hamilton, Ontario, L8S 4M1 CANADA
  e-mail: marcy@gemini.physics.mcmaster.ca

- Mr Pascal Manuel
  School of Physics and Astronomy
  University of St Andrews
  St Andrews, Fife, KY16 9SS, UK
  e-mail: pm10@st-and.ac.uk

- Mr Emilio Manzanares-Papayanopoulos
  Chemistry Department
  University of Sheffield
  Brookhill, Sheffield S3 7HF, UK
  e-mail: chp95em@sheffield.ac.uk

- Dr Yasuyuki Matsuda
  Muon Science Lab.
  RIKEN, Hirosawa 2-1
  Wako, Saitama, 351-0198 JAPAN
  e-mail: matsuday@riken.go.jp

- Mr Piotr Mietniowski
  Dept of Solid State Physics
  Univ of Mining and Metallurgy
  Av. Mickiewicza 30
  30-059 Cracow, POLAND
  e-mail: mietniow@uci.agh.edu.pl

- Mr Roger Miller
  University of British Columbia
  TRIUMF
  4004 Westbrook Mall
  Vancouver, BC V6T 2A3, CANADA
  e-mail: miller@physics.ubc.ca

- Dr Luis Morellon
  Dpto de Fisica de la Materia Condensada
  Universidad de Zaragoza
  Pedro Cerbuna 12, 50009 Zargoza
  SPAIN
  e-mail: morellon@posta.unizar.es

- Dr Elvezio Morenzoni
  Paul Scherrer Institut
  Würenlingen and Villigen
  CH-5232 Villigen PSI
  SWITZERLAND
  e-mail: elvezio.morenzoni@psi.ch

- Professor Ken Nagamine
  Meson Science Laboratory
  Institute of Materials Structure Science
  High Energy Accelerator Research Organisation
  Tsukuba, Ibaraki 305-0198
  JAPAN
  e-mail: kanetada.nagamine@kek.jp

- Dr Feodor Ogrin
  School of Physics and Astronomy
  University of St Andrews
  St Andrews, KY16 9SS, UK
  e-mail: fo1@st-and.ac.uk

- Professor Brian Rainford
  Department of Physics
  University of Southampton
  Southampton, S09 5NH, UK
  e-mail: bdr@phys.soton.ac.uk

- Professor Migg Roduner
  Institut für Physikalische Chemie
  Universität Stuttgart
  Pfaffenwaldring 55
  D-70569 Stuttgart, GERMANY
  e-mail: Emil.Roduner@psi.ch

- Mr Zaher Salman
  Physics Faculty
  Technion-Israel Institute of Technology
  Technion City, Haifa 32000, ISRAEL
  e-mail: zaher@minerva1.technion.ac.il

- Dr Robert Scheuermann
  Physikalisches Institut de Universitaet Heidelberg
  Gruppe ANP/Jungmann
  Philosophenweg 12, 69120
  Heidelberg, GERMANY
  e-mail: scheuermann@psi.ch

- Dr Alex Schenck
  Institute of Particle Physics
  ETHZ, IPP/ETHZ, WLGA/C21
  5232 Villigen-PSI, SWITZERLAND
  e-mail: Alexander.Schenck@psi.ch

- Mr Toni Shiroka
  Dipartimento Di Fisica
  University of Parma
  Viace Delle Scienze
  C-43100 Parma, ITALY
  e-mail: toni@prix7.pr.infn.it

- Dr Vyacheslav Storchak
  Kurchatov Institute
  Kurchatov Square, 1
  Moscow 123182, RUSSIA
  e-mail: storchak@dnuc.polyn.kiae.su

- Dr John Stride
  Laboratoire Lëon Brillouin
  CEA-Saclay
  91191 Gif-sur-Yvette Cedex
  FRANCE
  e-mail: stride@llb.saclay.cea.fr

- Mr Robert Tarragona
  Columbia University
  F28 PUPIN, Mailcode 9314
  538 W 120th Street, New York
  NY 10027 USA
  e-mail: rt120@columbia.edu

- Mr Konrad Traeger
  Physikalisches Institut de Universaet Heidelberg
  Gruppe ANP/Jungmann
  Philosophenwag 12, 69120
  Heidelberg, GERMANY
  e-mail: traeger@physi.uni-heidelberg.de

- Mr Daniel Ucko
  University College London
  Gower Street, London WC1E 6BT, UK
  e-mail: d.ucko@ucl.ac.uk

- Professor Tomo Uemura
  Physics Department
  Columbia University
  538 West 120th St
  New York, NY 10027, USA
  e-mail: tomo@kirby.phys.columbia.edu

- Mr Rui Vilao
  Physics Department
  University of Coimbra
  P-3000 Coimbra, PORTUGAL
  e-mail: ruivilao@gemini.ci.uc.pt

- Mr Alexey Volkov
  JINR, Leningradskaya, 10
  Dubna, Moscow Region, RUSSIA
  e-mail: alvolk@nusun.jinr.ru

- Mrs Yan Wang
  Physics Department
  UMIST, Manchester, M60 1QD UK
  e-mail: yan.wang@stud.umist.ac.uk

- Dr Maciej Wiesner
  Institute of Physics
  Mickiewicz University
  Umultowska Street 85
  61-614 Poznan, POLAND
  e-mail: mwiesner@main.amu.edu.pl

- Dr Piotr Wisniewski
  Onuki Laboratory
  Graduate School of Science
  Osaka University, Toyonaka
  Osaka 560-0043, JAPAN
  e-mail: wisniew@int.pan.wroc.pl

- Mr Darius Zajac
  University of Mining and Metallurgy
  Department of Solid State Physics
  30-059 Cracow, POLAND
  e-mail: 5zajac_d@novell.ftj.agh.edu.pl

- Mr Ion-Sorin Zgura
  Institute of Space Sciences
  Atomistilor Street
  N0101, Bucharest-Magurele
  PO Box MG-6,RO 76900, ROMANIA
  e-mail: zis@venus.ifa.ro

- Dr Jan Zukrowski
  University of Mining and Metallurgy
  Department of Solid State Physics
  30-059 Cracow, POLAND
  e-mail: zukrow@uci.agh.edu.pl

Index

MUON SCIENCE
Muons in Physics, Chemistry and Materials

51st Scottish Universities Summer School in Physics

EDITORS
S. L. LEE
S. H. KILCOYNE
R. CYWINSKI

The Scottish Universities Summer Schools in Physics have been held every year since 1960. The purpose of these schools is to contribute to the dissemination of advanced knowledge and the formation of contacts among scientists from different countries.

The lecturers at these schools are all international experts in their subject. Their brief is to present an up-to-date survey of current research in their own field in the form of a coherent series of lectures at a level suitable for students who are normally in their second or third postgraduate year.

Muon science is rapidly assuming a central role in scientific and technological studies of the solid state within the disciplines of physics, chemistry and materials science. This book is a collection of lectures delivered at SUSSP 51, the aim of which is to formalize and publicize recent key developments in both theoretical and experimental aspects of muon spin relaxation, rotation and resonance. The contributors are internationally renowned experts in muon instrumentation and applications of muon science, who cover topics which include: muon production; beamlines and instrumentation; muonium chemistry; muon catalysed fusion; fundamental muon physics; ultra-cold muons; magnetism; superconductivity; diffusion; semiconductors; simulations and data analysis. The book, which is aimed primarily at a graduate audience, assumes no prior expertise in muon science, and takes the reader through from introductory material to the latest developments in the field. Consistent notation and nomenclature are maintained throughout, with cross-referencing and continuity between the contributions. The book provides an excellent introduction to both new and experienced muon beam scientists wishing to develop their knowledge and understanding of the subject.

ISBN 0-7503-0630-0

9 780750 306300 >

Institute of Physics Publishing
Bristol and Philadelphia